INTERNATIONAL JOURNAL FOR NUMERICAL METHODS IN FLUIDS
Int. J. Numer. Meth. Fluids 2008; **58**:307–317
Published online 14 January 2008 in Wiley InterScience (www.interscience.wiley.com). DOI: 10.1002/fld.1723

Remarks on the links between low-order DG methods and some finite-difference schemes for the Stokes problem

P. D. Minev*, †

Department of Mathematical & Statistical Sciences, University of Alberta, Edmonton, Alta., Canada T6G 2G1

SUMMARY

In this paper we demonstrate that some well-known finite-difference schemes can be interpreted within the framework of the local discontinuous Galerkin (LDG) methods using the low-order piecewise solenoidal discrete spaces introduced in (*SIAM J. Numer. Anal*. 1990; **27**(6): 1466–1485). In particular, it appears that it is possible to derive the well-known MAC scheme using a first-order Nédélec approximation on rectangular cells. It has been recently interpreted within the framework of the Raviart–Thomas approximation by Kanschat (*Int. J. Numer. Meth. Fluids* 2007; published online). The two approximations are algebraically equivalent to the MAC scheme, however, they have to be applied on grids that are staggered on a distance $h/2$ in each direction. This paper also demonstrates that both discretizations allow for the construction of a divergence-free basis, which yields a linear system with a 'biharmonic' conditioning. Both this paper and Kanschat (*Int. J. Numer. Meth. Fluids* 2007; published online) demonstrate that the LDG framework can be used to generalize some popular finite-difference schemes to grids that are not parallel to the coordinate axes or that are unstructured. Copyright © 2008 John Wiley & Sons, Ltd.

Received 7 September 2007; Revised 13 November 2007; Accepted 20 November 2007

KEY WORDS: Navier–Stokes equations; discontinuous Galerkin methods; finite-difference methods

1. INTRODUCTION

This study was inspired by the paper of Kanschat [1], which discusses the interpretation of one of the earliest schemes used for the discretization of the Stokes equations, the MAC scheme, as a discontinuous Galerkin (DG) method. In that paper, it was shown that using a proper quadrature, the first-order local discontinuous Galerkin (LDG) method of Cockburn *et al*. [2] can be made algebraically equivalent to the MAC scheme. This method is based on the well-known H^{div}-conforming Raviart–Thomas RT_0 element. In fact, the analogy between the RT_0 and the MAC

*Correspondence to: P. D. Minev, Department of Mathematical & Statistical Sciences, University of Alberta, Edmonton, Alta., Canada T6G 2G1.
†E-mail: minev@ualberta.ca

Contract/grant sponsor: National Science and Engineering Research Council of Canada; contract/grant number: 216926-07

spatial discretization has been pointed out by Girault and Lopez [3] who interpreted the MAC scheme as a mixed H^{div}-conforming finite element method. However, the DG setting seems to make the analogy more direct. The MAC method has also been interpreted and analyzed as a co-volume method in [4, 5], and as a classical continuous finite element method on staggered quadrilateral grids in [6].

In this paper we use discontinuous approximations based on the piecewise solenoidal discrete spaces introduced in [7] (see also [8]). We demonstrate that the piecewise-constant approximation for the velocity on a uniform rectangular grid and the C^0 piecewise linear approximation for the pressure on a uniform triangular grid produced by subdividing the rectangles with their diagonals yield a linear system equivalent to the system resulting from a finite-difference scheme proposed in [9, 10] (we denote it by KF). This finite-difference scheme is $O(h^2)$ consistent approximation of both the Laplace operator and the divergence/gradient operators. The latter scheme is also equivalent to the scheme proposed in [11], which we denote by BCG (up to the treatment of the boundary conditions). The higher-order locally solenoidal approximations are related to the so-called Nédélec spaces (see [12]) which are H^{curl}-conforming and are used mostly for the discretization of the Maxwell equations. The first-order approximation for the velocity and the C^0 piecewise bilinear approximation for the pressure on a uniform rectangular grid yield a scheme that can be made algebraically equivalent to the MAC scheme. It is remarkable that the discretization of the Laplace operator is $O(h^4)$ consistent and it is the discretization of the gradient/divergence that reduces the overall consistency to second order. Thus, both schemes are $O(h^2)$ accurate (in a discrete maximum norm) and so the solution can be re-interpolated to obtain a fully second-order (in an L^2 norm) approximation. Standard theory with such interpolation spaces cannot be expected to yield that high convergence rates; therefore, this hints at a possible superconvergence on uniform grids. Note that the first scheme does not satisfy the inf–sup stability condition. However, the pressure space contains only one spurious checkerboard mode, which can be easily eliminated.

These two DG discretizations can be used to generalize the corresponding finite-difference methods to unstructured grids or grids with non-matching nodes. The generalization of the first scheme to 3D is straightforward. The generalization of the second scheme to 3D involves degrees of freedom for the velocity on the edges rather than faces of the elements and follows the same idea as the generalization of the Nédélec elements.

2. THE DG SETTING

For simplicity of the presentation, we consider only the discretization of the steady Stokes equations on a uniform rectangular grid $\mathscr{G}_h$ with a stepsize h in $\Omega=(0,1)\times(0,1)$ with Dirichlet boundary conditions on the entire domain boundary. Using various numerical fluxes, the schemes can be easily extended to the Navier–Stokes equations and generalized to non-rectangular domains. As already mentioned above, the discretization spaces for the velocity are constructed following the idea in [7].

2.1. Scheme 1

We will start with the scheme based on a piecewise-constant approximation for the velocity. The discrete velocity space is, therefore, defined as $\mathbf{V}_h=\{(u_h,v_h)^{\mathrm{T}}\in\mathbf{L}^2(\Omega);\, u_h=\mathrm{const},\, v_h=\mathrm{const}|_s \forall s\in\mathscr{G}_h\}$. It is clearly spanned by the lowest-order piecewise divergence-free functions

DOI: 10.1002/fld

introduced in [7]. With this choice for the velocity discretization, the most natural choice for the pressure is a continuous approximation. We used pyramidal basis functions that are linear on each elemental edge and piecewise linear in each quadrilateral element. The basis function for the pressure associated with a given node $(i+\frac{1}{2}, j+\frac{1}{2})$ is represented in Figure 1. Since the velocity is piecewise constant, we have to employ the DG apparatus in order to discretize the Laplacian. Note that if we integrate by parts the usual Galerkin divergence operator, we will obtain a consistent discretization for the divergence because the pressure approximation is in H^1. To this end, we use the following bilinear forms for the discretization of the Laplacian (see [2]):

$$a_h(\mathbf{u}_h, \mathbf{v}_h) = -\sum_{e \in \mathscr{E}^{\mathrm{I}}} \frac{k}{h} [[\mathbf{u}_h \mathbf{n}]][[\mathbf{v}_h \mathbf{n}]] \quad \forall \mathbf{u}_h, \mathbf{v}_h \in \mathbf{V}_h \tag{1}$$

where $\mathscr{E}^{\mathrm{I}}$ is the set of all internal elemental edges and $[[\mathbf{w}_h \mathbf{n}]] = \mathbf{w}_h^+ \mathbf{n}^+ + \mathbf{w}_h^- \mathbf{n}^-$ denotes the jump of the corresponding quantity in the normal to this edge direction. Note that this follows exactly from the bilinear forms for the Laplacian used in the methods of [2, 7] in the present case of piecewise constant basis for the velocity and provided that the boundary conditions on both components of the velocity are imposed strongly (see Remark 2.1). The divergence (and subsequently the gradient) operator is defined by

$$b_h(\mathbf{u}_h, q_h) = -\int_\Omega \mathbf{u}_h \nabla q_h \, \mathrm{d}\Omega \tag{2}$$

As we already mentioned, this DG formulation is equivalent to two finite-difference schemes proposed in the past: the KF and BCG schemes. The difference occurs only around the boundary of the domain and once the equivalence with one of the schemes is shown, it is straightforward to do the same for the other scheme with a proper imposition of the boundary conditions (see Remark 2.1). This is why we will show only the equivalence with the KF scheme. Suppose that we have N elements in the grid in each direction and denote the centroidal values of the x- and y-components of the velocity by $u_{i,j}, v_{i,j}, i, j = 1, \ldots, N$. Suppose also that $\mathbf{u}_h = \sum_{i,j=1}^{N} (u_{i,j}, v_{i,j})^{\mathrm{T}} \xi_{i,j}$ with $\xi_{i,j}$

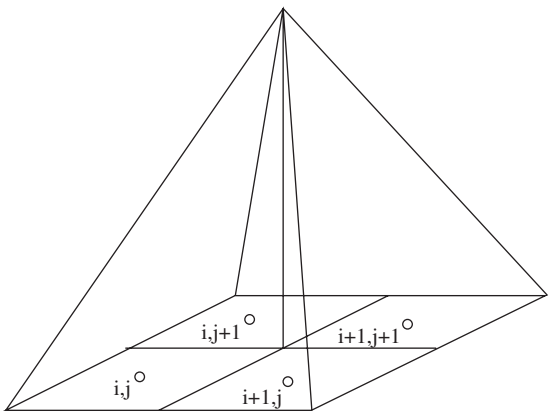

Figure 1. A pressure basis function in an internal pressure node $i+\frac{1}{2}, j+\frac{1}{2}$; the velocity nodes are marked with $\circ$.

DOI: 10.1002/fld

being the characteristic function of the square element centered at point i, j. Then (1) yields, for $k=1$, the following discretization for the Laplacian of the x-component of the velocity at point i, j (we clearly need to take $\mathbf{v}_h=(\xi_{i,j},0)^{\mathrm{T}}$):

$$a_h(\mathbf{u}_h,\mathbf{v}_h)=u_{i+1,j}+u_{i-1,j}+u_{i,j+1}+u_{i,j-1}-4u_{i,j} \tag{3}$$

This, up to the factor h^2, is exactly the five-point stencil finite difference used in the KF scheme. The factor h^2 appears because the right-hand side vector will contain an integral of the source term. Equation (2) yields the following finite-difference approximation of the divergence at point $(i+1/2, j+1/2)$ (we need to choose q_h to be the function shown in Figure 1):

$$b_h(\mathbf{u}_h,q_h)=\frac{h}{2}(u_{i+1,j+1}-u_{i,j+1}+u_{i+1,j}-u_{i,j}+v_{i,j+1}-v_{i,j}+v_{i+1,j+1}-v_{i+1,j}) \tag{4}$$

This is clearly, up to a factor h^2, the second-order consistent approximation for the divergence used in KF. The approximation for the x-component of the pressure gradient at point (i, j) is given by

$$\frac{h}{2}(p_{i+1/2,j+1/2}-p_{i-1/2,j+1/2}+p_{i+1/2,j-1/2}-p_{i-1/2,j-1/2}) \tag{5}$$

which is clearly a second-order finite-difference approximation to the gradient. Unfortunately, this combination of velocity/pressure approximation is not inf–sup stable. Indeed, the averaging operator allows to have a non-zero (non-constant) pressure with a zero gradient, however, it is easy to see that there is only one global spurious checkerboard mode, and it is not difficult to filter it out. It is also clear that the piecewise-constant approximation for the velocity cannot yield higher than first-order accuracy in the L^2 norm. On the other hand, the equivalent finite-difference scheme is second-order accurate, which indicates a pointwise superconvergence of the solution.

Remark 2.1

In case of the KF scheme, the velocities are located in the vertices of a regular grid (ih, jh) and the pressure is located in the cell centers $((i+\frac{1}{2})h, (j+\frac{1}{2})h)$. In order to reproduce algebraically the linear system of the KF discretization from the DG formulation, we need to place the vertices of the finite elements in the pressure nodes so that the velocity nodes are placed in the centroids of the finite elements. In addition, in order to impose the velocity boundary conditions strongly, we need to align the centroids of the first layer of finite elements around the boundary Γ with the boundary nodes and extend the pressure nodes with one layer of 'ghost' nodes around each portion of the boundary (see Figure 2). The outside layer of 'ghost' pressure nodes is not needed to compute the pressure gradient (and to test the incompressibility constraint) because the velocity at the boundary velocity nodes is prescribed, i.e. the pressure gradient in these nodes is not required for its computation.

The BCG scheme places the velocity nodes in the cell centers; therefore, in order to reproduce it algebraically with the DG formulation, it is necessary to use the finite-difference cells as DG finite elements. Then, it imposes the Dirichlet boundary conditions by introducing a layer of 'ghost' velocity points around each portion of the boundary Γ and using an averaging operator. This can be reproduced in the DG formulation by introducing a layer of finite elements around each portion of the boundary (see Figure 2). Then, the newly introduced velocity degrees of freedom can be determined from the condition that the linear interpolant in the x-direction for the left and right portions of the boundary and in the y-direction for the top and bottom portions of the boundary

DOI: 10.1002/fld

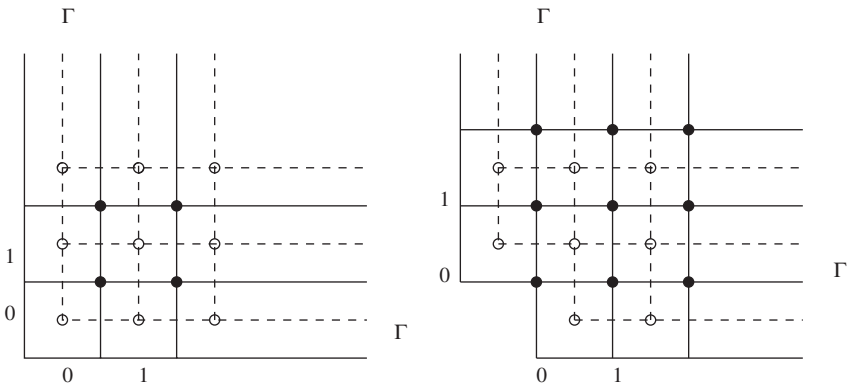

Figure 2. The KF (left) and BCG (right) grids at the lower left corner of the domain. The DG finite element grid is marked by a solid line and the finite-difference grid for the velocity is marked by a dashed line. The velocity nodes are marked by ∘ and the pressure nodes by •.

satisfies the boundary conditions. This defines essentially a second-order averaging operator. Again, the additional layer of 'ghost' pressure degrees of freedom is not used because the pressure gradient in the additional layer of velocity nodes is not needed. Of course, the DG formulation offers also the alternative of a weak imposition of the boundary conditions as discussed by Kanschat [1] in case of the MAC scheme.

2.2. *Scheme 2*

In order to construct the other scheme, we need to use the higher degree divergence-free polynomial vectors introduced in [7]. On the standard rectangle $[0,1]^2$, they are spanned by $(1,0)^{\mathrm{T}}$, $(0,1)^{\mathrm{T}}$, $(y,0)^{\mathrm{T}}$, $(0,x)^{\mathrm{T}}$ and $(x,-y)^{\mathrm{T}}$. It appears that if we choose only the subspace spanned by $(y,0)^{\mathrm{T}}$, $(1-y,0)^{\mathrm{T}}$, $(0,x)^{\mathrm{T}}$, $(0,1-x)^{\mathrm{T}}$, we obtain the local representation of the Nédélec space of first kind on a rectangle. Therefore, the fifth local function is not necessary to obtain a consistent approximation of functions in H^{curl}. Thus, the velocity approximation is sought in

$$\mathbf{V}_h = \{\mathbf{v}_h \in H^{\mathrm{curl}}; \mathbf{v}_h|_s \in \mathrm{span}\{(y,0)^{\mathrm{T}}, (1-y,0)^{\mathrm{T}}, (0,x)^{\mathrm{T}}, (0,1-x)^{\mathrm{T}}\}, \forall s \in \mathscr{G}_h\} \tag{6}$$

In this space, the x-component of the velocity is cellwise constant (and discontinuous) in the x-direction and cellwise linear (and continuous) in the y-direction. The unknowns associated with the approximation in it are the average values of the tangential components of the velocity on each edge of a rectangular cell. Since we consider an uniform grid, it is quite clear that in the dual grid produced by connecting the centroids of the rectangles of the Nédélec grid, these unknowns will play the same role as the unknowns of the MAC scheme on the dual grid, i.e. they are normal velocities in the edge midpoints of the dual rectangles. Thus in some sense the present approximation is 'dual' to the MAC scheme. The pressure space that is usually associated with the Nédélec basis is continuous, and the weak form of the divergence operator is given by (2). In this case, we use the usual piecewise bilinear Q_1 approximation

$$Q_h = \left\{ q_h \in H^1; q_h|_s \in \mathrm{span}(1, x, y, xy), \forall s \in \mathscr{G}_h; \int_\Omega q_h = 0 \right\} \tag{7}$$

DOI: 10.1002/fld

The functions used to construct the velocity basis have a prismatic shape and they are equal to 1 on the entire edge with which they are associated, and to 0 on the two neighboring edges parallel to it. In terms of the notations in Figure 3, the basis function $\phi_{i,j-1/2}(y)$ associated with the edge centered at $i, j-\frac{1}{2}$ is linear on each cell and equal to one along the edge between the points $i, j-1$ and i, j. It also equals 0 along the edges from $i-1, j-1$ to $i-1, j$, and from $i+1, j-1$ to $i+1, j$ as well as anywhere outside the rectangles centered at $i-\frac{1}{2}, j-\frac{1}{2}$ and $i+\frac{1}{2}, j-\frac{1}{2}$ (see Figure 3). On vertical edges, these functions approximate the vertical components of the velocity and on horizontal edges they approximate the horizontal component. Hence, the velocity in the cell centered at $i-\frac{1}{2}, j-\frac{1}{2}$ is given by

$$\mathbf{u}(x, y)|_{i-1/2,j-1/2} = \begin{bmatrix} u_{i-1/2,j-1}\phi_{i-1/2,j-1}(y) + u_{i-1/2,j}\phi_{i-1/2,j}(y) \\ v_{i-1,j-1/2}\phi_{i-1,j-1/2}(x) + v_{i,j-1/2}\phi_{i,j-1/2}(x) \end{bmatrix} \tag{8}$$

Since the basis for the velocity is no longer cellwise constant, (1) should be augmented as follows (see [2]):

$$a_h(\mathbf{u}_h, \mathbf{v}_h) = \sum_{s\in\mathscr{G}_h} \int_s \nabla\mathbf{u}_h : \nabla\mathbf{v}_h - \sum_{e\in\mathscr{E}^{\mathrm{I}}} \frac{k}{h}[[\mathbf{u}_h\mathbf{n}]][[\mathbf{v}_h\mathbf{n}]]h \quad \forall\mathbf{u}_h, \mathbf{v}_h \in \mathbf{V}_h \tag{9}$$

If we now choose $\mathbf{v}_h = (\phi_{i-1/2,j}(y), 0)^{\mathrm{T}}$ and $k=1$, this bilinear form yields the following approximation to the Laplacian of the horizontal velocity component at $i-1/2, j$:

$$\begin{aligned} a_h(\mathbf{u}_h, \mathbf{v}_h) = \tfrac{1}{6}(&-20u_{i-1/2,j} + 4(u_{i-3/2,j} + u_{i+1/2,j} + u_{i-1/2,j-1} + u_{i-1/2,j+1}) \\ &+ (u_{i-3/2,j-1} + u_{i+1/2,j-1} + u_{i+1/2,j+1} + u_{i-3/2,j+1})) \end{aligned} \tag{10}$$

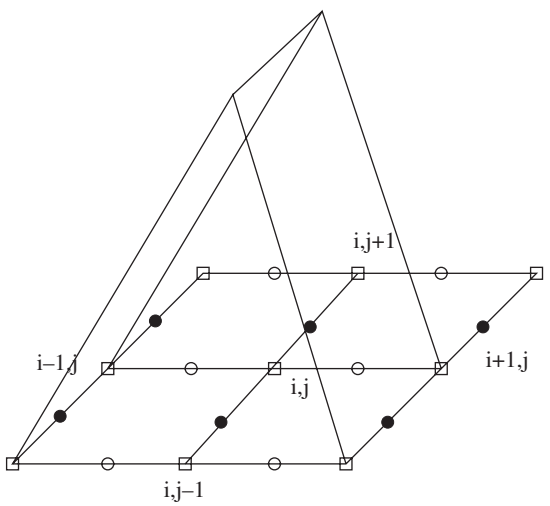

Figure 3. The velocity basis function corresponding to the vertical velocity component at $i, j-\frac{1}{2}$. Pressure nodes are marked with □, the horizontal velocity nodes are marked with ○ and the vertical velocity nodes with •.

DOI: 10.1002/fld

which is a fourth-order accurate finite-difference scheme. It is also an elementary exercise to compute the finite-difference stencil for the approximation of the divergence. Choosing $q_h = q_{i,j}(x, y)$ in (2), we obtain

$$\begin{aligned} b_h(\mathbf{u}, q_{i,j}) = \frac{h}{6}(4(u_{i+1/2,j} - u_{i-1/2,j} + v_{i,j+1/2} - v_{i,j-1/2}) + u_{i+1/2,j+1} \\ - u_{i-1/2,j+1} + u_{i+1/2,j-1} - u_{i-1/2,j-1} + v_{i-1,j+1/2} \\ - v_{i-1,j-1/2} + v_{i+1,j+1/2} - v_{i+1,j-1/2}) \end{aligned} \tag{11}$$

This is a finite-difference approximation to the divergence at i, j in which the x and y central difference approximations to the first derivatives are averaged according to the Simpson's rule in the direction orthogonal to the direction of the derivative. Therefore, this is a $O(h^2)$ consistent approximation for the divergence. Subsequently, the pressure gradient approximation is also $O(h^2)$ consistent. If both components of the boundary condition are imposed weakly, then $\nabla Q_h \subset \mathbf{V}_h$ and it is easy to show (see [13, p. 179]) that this pair of velocity/pressure approximation spaces satisfies the inf–sup stability condition and thus the pressure computed with the corresponding finite-difference scheme does not suffer of spurious modes. If the boundary condition is imposed strongly, the pressure stability cannot be guaranteed. The stencil of this finite-difference scheme is larger than the stencil of the classical MAC scheme. However, using the trick of [1] (see Lemma 4.1 of [1]), the finite-difference approximation of Laplacian (10) can be reduced to the classical five-point approximation. The divergence approximation (11) can be reduced to the classical central difference approximation of the MAC scheme using an inexact trapezoidal integration in each direction to approximate the integral in (2), which yields

$$\hat{b}_h(\mathbf{u}, q_{i,j}) = h(u_{i+1/2,j} - u_{i-1/2,j} + v_{i,j+1/2} - v_{i,j-1/2}) \tag{12}$$

where $\hat{b}_h$ denotes the approximation to b_h obtained with the inexact trapezoidal quadrature rule. Note that both finite-difference approximations of the divergence, (11) and (12), have the same $O(h^2)$ consistency. However, the pressure gradient discretization that follows from (12) has a trivial null space; therefore, the pressure approximation is guaranteed to be stable. The scheme comprised by (10) as a discretization of the Laplacian and (12) (or its transposed) as a discretization of the divergence (or the gradient) operators is algebraically equivalent to the scheme that results from the divergence-free DG method discussed by Kanschat [1], which is based on the lowest-order Raviart–Thomas (RT_0) quadrilaterals, however applied on the dual grid. From the approximation point of view, however, the two approaches are quite different. The first important difference is that the Nédélec approximation is H^{curl} conforming; therefore, it can be used as a conforming approximation for the Stokes problem in the following non-standard formulation:

$$\begin{aligned} -\nabla\times\nabla\times\mathbf{u} - \nabla p &= \mathbf{f} \quad \text{in } \Omega \\ \nabla\cdot\mathbf{u} &= 0 \quad \text{in } \Omega \\ \mathbf{u} &= 0 \quad \text{on } \partial\Omega \end{aligned} \tag{13}$$

It is obtained by applying the Helmholtz decomposition $\nabla^2\mathbf{u} = \nabla\nabla\cdot\mathbf{u} - \nabla\times\nabla\times\mathbf{u}$ to the usual form of the Stokes problem and taking into account the incompressibility constraint. The weak

DOI: 10.1002/fld

formulation associated with this problem reads: Find $\mathbf{u} \in H_0^{\mathrm{curl}}(\Omega)$, $\mathbf{u}.\mathbf{n}_{|\Gamma} = 0$ and $p \in H^1(\Omega)$, $\int_\Omega p = 0$ s.t.

$$\begin{aligned} (\nabla \times \mathbf{u}, \nabla \times \mathbf{v}) + (\nabla p, \mathbf{v}) &= (\mathbf{f}, \mathbf{v}) \quad \forall \mathbf{v} \in H_0^{\mathrm{curl}}(\Omega), \quad \mathbf{v}.\mathbf{n}_{|\Gamma} = 0 \\ -(\nabla q, \mathbf{u}) &= 0 \quad \forall q \in H^1(\Omega) \quad \text{s.t.} \quad \int_\Omega q = 0 \end{aligned} \tag{14}$$

It is clear that the solution of the standard Stokes problem

$$\begin{aligned} \nabla^2 \mathbf{u} - \nabla p &= \mathbf{f} \quad \text{in } \Omega \\ \nabla \cdot \mathbf{u} &= 0 \quad \text{in } \Omega \\ \mathbf{u} &= 0 \quad \text{on } \partial\Omega \end{aligned} \tag{15}$$

satisfies (13) but the converse is not necessarily true. The solution of (13) satisfies (15) only if it is regular enough and so, it is a kind of a generalization of the Stokes problem. Note, that if applied to (13) the Nédélec approximation is fully conforming. However, the strong imposition of the normal component of the velocity boundary condition on to the Nédélec approximation space is non-trivial. One possibility is to use a grid similar to the grid of the KF scheme (see Figure 4) and slightly modify the basis in the elements intersected by the boundary. Let us consider as an example the element in Figure 4 whose centroid has integer coordinates $(1, 0)$. Then, the imposition of the normal components of the boundary condition on the nodes $(\frac{1}{2}, 0)$ and $(\frac{3}{2}, 0)$ is straightforward. The tangential boundary condition can be imposed strongly on the velocity space if the horizontal component of the velocity is spanned by $\phi_{1,1/2} - \phi_{1,-1/2}$. If the velocity boundary condition is imposed strongly, then the divergence operator in (14) should be computed with an inexact quadrature, as discussed above, in order to guarantee the inf–sup stability of the formulation. A possible alternative is to impose the boundary conditions weakly (see [1] for example) and in such case the pressure gradient is spanned by the velocity basis and therefore the inf–sup stability argument of [13] applies.

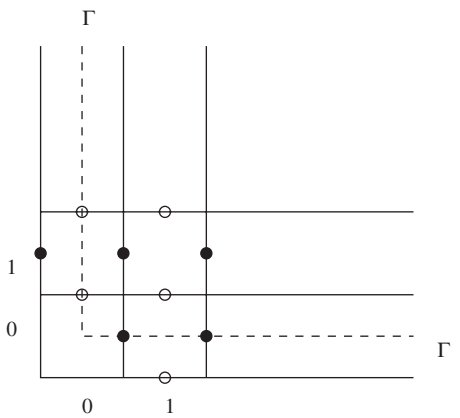

Figure 4. An example of a finite element grid around the lower left corner of the domain, which can be used for a strong imposition of both components of the velocity boundary condition; the horizontal velocity nodes are marked with ∘ and the vertical velocity nodes with •.

DOI: 10.1002/fld

The other difference between the Nédélec and Raviart–Thomas approximations is that the advection terms in the full Navier–Stokes equations must be treated differently. The normal traces of the Nédélec approximant are discontinuous across the element edges, which requires to incorporate a stabilization flux, e.g. a Godunov flux, in the discretization. The RT_0 approximant is essentially continuous in the normal direction, and it can be used to build a pointwise divergence-free velocity as proposed in [2].

Remark 2.2
Since the discretization of Laplacian (10) is fourth-order consistent and the discretizations of divergence (11) or (12) are second-order consistent, it can be expected that Scheme 2 is superconvergent for both the velocity and the pressure provided that the normal component of the boundary condition is imposed properly. For various ways to improve the boundary condition discretization, the reader is referred to [14, pp. 151–153].

2.3. Divergence-free basis

The reduced approximation to divergence (12) allows for an easy construction of a divergence-free basis. Consider the cell centered at $i+\frac{1}{2}, j+\frac{1}{2}$ (see Figure 3). Then the following function

$$\boldsymbol{\omega}_{i+1/2,j+1/2}=\begin{bmatrix}\phi_{i+1/2,j}\\0\end{bmatrix}+\begin{bmatrix}0\\\phi_{i+1,j+1/2}\end{bmatrix}-\begin{bmatrix}\phi_{i+1/2,j+1}\\0\end{bmatrix}-\begin{bmatrix}0\\\phi_{i,j+1/2}\end{bmatrix} \tag{16}$$

satisfies $\hat{b}_h(\boldsymbol{\omega}_{i+1/2,j+1,2}, q_{i+k,j+l})=0$, where $k,l=0,\pm 1$. It is clearly a linear combination of Nédélec basis functions. According to the Euler formula, the number of cells equals the difference in the number of edges and the number of nodes in the grid minus 1. Since with each cell we can associate exactly one such divergence-free function, the algebraic system that follows from the discretization of the Stokes equations with this basis must be equivalent, up to the treatment of the normal component of the boundary conditions, to the system produced by first approximating the momentum equation with the Nédélec basis (the number of equations equals the number of edges); then, explicitly resolving each of the equations of the reduced incompressibility constraint (12) (the number of equations equals the number of nodes minus one). The boundary conditions for the new degrees of freedom associated with the divergence-free basis can be imposed strongly by introducing an additional layer of cells on the outside of the boundary. Then, the tangential component of the boundary condition is imposed in the midpoint of each boundary edge of a cell and the normal component is imposed in the boundary vertices. In case of domains that are not simply connected, the divergence-free approach is more complicated and may require the use of non-local basis functions (see, for example, [15, p. 309]).

Similar to other discretizations based on a divergence-free approximation (see, for example, [16]), numerical results suggest that the resulting linear system has a condition number of the order of $O(h^{-4})$, which corresponds to a biharmonic problem. Nevertheless, the size of the system is much smaller and, thus, this approach is not entirely ruled out by the relatively bad conditioning. It could be particularly efficient in the case of the unsteady Navier–Stokes equations at high Reynolds numbers because the conditioning of the system in such case can be expected to be better than $O(h^{-4})$ (closer to $O(h^{-2})$). Moreover, it is possible to design efficient preconditioners of a mutigrid type for example.

DOI: 10.1002/fld

Remark 2.3
The construction of a 3D divergence-free basis is a little more involved and can be done similarly to the one done for the non-conforming Crouzeix–Raviart element. The reader is referred to [15] and the references therein for the latter approach.

Remark 2.4
Note that a similar divergence-free basis can be constructed for the RT_0 method of [1]. While in (16), the basis is comprised by the sum of all (tangential) basis functions on the edges of a given element (taken in a anti-clockwise direction), the RT_0 basis requires to take the sum of all the (normal) basis functions corresponding to all edges connected to a given node (taken in an anti-clockwise direction).

3. CONCLUSIONS

The main conclusion of this paper is that three well-known finite-difference schemes can be produced using a piecewise divergence-free approximation within the framework of the LDG method. This analogy allows for an easy generalization of these schemes to unstructured grids or grids whose edges are not parallel to the coordinate axes. It also allows to construct finite-difference schemes on grids with non-matching nodes. The approximation with first-degree polynomial piecewise divergence-free vectors can be made algebraically equivalent to the MAC scheme, and therefore to the lowest-order Raviart–Thomas approximation, if employed on a dual grid obtained by connecting the centroids of the MAC cells. In fact, from approximation standpoint it is equivalent to the lowest-order Nédélec approximation on quadrilaterals. The standard finite element theory does not yield proper error estimates for these schemes and one possibility could be to obtain a superconvergence result for the nodal values of the solution and then use it to obtain optimal error estimates.

The method based on the Nédélec approximation allows for an easy construction of a divergence-free basis, which can be used for the discretization of both the Stokes problem and the time-harmonic Maxwell equations at vanishing wave numbers. The numerical evidence confirms that the matrix resulting from this basis has a biharmonic conditioning, however, the size of the linear system is significantly smaller than the original system. It is also positive definite, as opposed to the indefinite saddle-point system resulting from the traditional approximation in primitive variables. Thus, it can be advantageous to use directly the divergence-free basis, particularly in the case of high Reynolds number flows. A similar idea can be applied to develop a divergence-free basis from the 2D Raviart–Thomas element in the context of the scheme developed in [17]. The development of a divergence-free basis in 3D in both the Nédélec and Raviart–Thomas cases is more involved but certainly possible. There is no much done in this direction and it is probably worth exploring the possibility to design efficient preconditioners for the resulting linear systems.

ACKNOWLEDGEMENT

The author would like to acknowledge the helpful comments of Guido Kanschat on the first version of this article.

DOI: 10.1002/fld

REFERENCES

1. Kanschat G. Divergence-free discontinuous Galerkin schemes for the Stokes equations and the MAC scheme. *International Journal for Numerical Methods in Fluids* 2007; DOI: 10.1002/fld.1556.
2. Cockburn B, Kanschat G, Schötzau D. A locally conservative LDG method for the incompressible Navier–Stokes equations method for the incompressible Navier–Stokes equations. *Mathematics of Computation* 2005; **74**:1067–1095.
3. Girault V, Lopez H. Finite element error estimates for the MAC scheme. *IMA Journal of Numerical Analysis* 1996; **16**:347–379.
4. Nicolaides RA. Analysis and convergence of the MAC scheme I. The linear problem. *SIAM Journal on Numerical Analysis* 1992; **29**(6):1579–1591.
5. Nicolaides RA, Wu X. Analysis and convergence of the MAC scheme II. The Navier–Stokes equations. *Mathematics of Computation* 1996; **65**:29–44.
6. Han H, Wu X. A new mixed finite element formulation and the MAC method for the Stokes equations. *SIAM Journal on Numerical Analysis* 1998; **35**(2):560–571.
7. Baker G, Jureidini W, Karakashian O. Piecewise solenoidal vector fields and the Stokes problem. *SIAM Journal on Numerical Analysis* 1990; **27**(6):1466–1485.
8. Karakashian O, Jureidini W. A nonconforming finite element method for the stationary Navier–Stokes equations. *SIAM Journal on Numerical Analysis* 1998; **35**(1):93–120.
9. Kuznetsov BG. Numerical methods for solving some problems of viscous liquid. *Fluid Dynamics Transactions* 1968; **4**:85–89.
10. Fortin M, Peyret R, Temam R. Calcul des ecoulements d'un fluide visqueux incompressible. *Journal de Mécanique* 1971; **10**:357–390.
11. Bell JB, Colella P, Glaz HM. A second order projection method for the incompressible Navier–Stokes equations. *Journal of Computational Physics* 1989; **85**:257–283.
12. Nédélec JC. A new family of mixed finite elements in R^3. *Numerische Mathematik* 1986; **50**:57–81.
13. Monk P. *Finite Element Methods for Maxwell's Equations.* Oxford Science Publications: Oxford, 2003.
14. Peyret R, Taylor TD. *Computational Methods for Fluid Flow.* Springer: Berlin, 1982.
15. Cuvelier C, Segal A, van Steenhoven A. *Finite Element Methods and the Navier–Stokes Equations*. D. Reidel: Dordrecht, 1986.
16. Brenner S. A nonconforming multigrid method for the stationary Stokes equations. *Mathematics of Computation* 1990; **55**:411–437.
17. Cockburn B, Kanschat G, Schötzau D. A note on discontinuous Galerkin divergence-free solutions of the Navier–Stokes equations. *Journal of Scientific Computing* 2007; **31**(1/2):61–73.